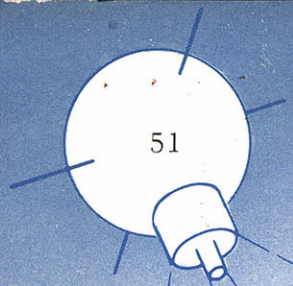

SATELLITE & MESOMETEOROLOGY RESEARCH PROJECT

Department of the Geophysical Sciences
The University of Chicago

FEATURES AND MOTIONS OF RADAR ECHOES ON PALM SUNDAY, 1965

by

Dorothy L. Bradbury and Tetsuya Fujita

(Chapter V of a Comprehensive Study of the Palm Sunday Tornadoes, 1965)

SMRP Research Paper

NUMBER 51

June 1966

MESOMETEOROLOGY PROJECT --- RESEARCH PAPERS

1.* Report on the Chicago Tornado of March 4, 1961 - Rodger A. Brown and Tetsuya Fujita

2.* Index to the NSSP Surface Network - Tetsuya Fujita

3.* Outline of a Technique for Precise Rectification of Satellite Cloud Photographs - Tetsuya Fujita

4.* Horizontal Structure of Mountain Winds - Henry A. Brown

5.* An Investigation of Developmental Processes of the Wake Depression Through Excess Pressure Analysis of Nocturnal Showers - Joseph L. Goldman

6.* Precipitation in the 1960 Flagstaff Mesometeorological Network - Kenneth A. Styber

7.** On a Method of Single- and Dual-Image Photogrammetry of Panoramic Aerial Photographs - Tetsuya Fujita

8. A Review of Researches on Analytical Mesometeorology - Tetsuya Fujita

9. Meteorological Interpretations of Convective Nephsystems Appearing in TIROS Cloud Photographs - Tetsuya Fujita, Toshimitsu Ushijima, William A. Hass, and George T. Dellert, Jr.

10. Study of the Development of Prefrontal Squall-Systems Using NSSP Network Data - Joseph L. Goldman

11. Analysis of Selected Aircraft Data from NSSP Operation, 1962 - Tetsuya Fujita

12. Study of a Long Condensation Trail Photographed by TIROS I - Toshimitsu Ushijima

13. A Technique for Precise Analysis of Satellite Data; Volume I - Photogrammetry (Published as MSL Report No. 14) - Tetsuya Fujita

14. Investigation of a Summer Jet Stream Using TIROS and Aerological Data - Kozo Ninomiya

15. Outline of a Theory and Examples for Precise Analysis of Satellite Radiation Data - Tetsuya Fujita

16. Preliminary Result of Analysis of the Cumulonimbus Cloud of April 21, 1961 - Tetsuya Fujita and James Arnold

17. A Technique for Precise Analysis of Satellite Photographs - Tetsuya Fujita

18. Evaluation of Limb Darkening from TIROS III Radiation Data - S.H.H. Larsen, Tetsuya Fujita, and W.L. Fletcher

19. Synoptic Interpretation of TIROS III Measurements of Infrared Radiation - Finn Pedersen and Tetsuya Fujita

20. TIROS III Measurements of Terrestrial Radiation and Reflected and Scattered Solar Radiation - S.H.H. Larsen, Tetsuya Fujita, and W.L. Fletcher

21. On the Low-level Structure of a Squall Line - Henry A. Brown

22. Thunderstorms and the Low-level Jet - William D. Bonner

23. The Mesoanalysis of an Organized Convective System - Henry A. Brown

24. Preliminary Radar and Photogrammetric Study of the Illinois Tornadoes of April 17 and 22, 1963 - Joseph L. Goldman and Tetsuya Fujita

25. Use of TIROS Pictures for Studies of the Internal Structure of Tropical Storms - Tetsuya Fujita with Rectified Pictures from TIROS I Orbit 125, R/O 128 - Toshimitsu Ushijima

26. An Experiment in the Determination of Geostrophic and Isallobaric Winds from NSSP Pressure Data - William Bonner

27. Proposed Mechanism of Hook Echo Formation - Tetsuya Fujita with a Preliminary Mesosynoptic Analysis of Tornado Cyclone Case of May 26, 1963 - Tetsuya Fujita and Robbi Stuhmer

28. The Decaying Stage of Hurricane Anna of July 1961 as Portrayed by TIROS Cloud Photographs and Infrared Radiation from the Top of the Storm - Tetsuya Fujita and James Arnold

29. A Technique for Precise Analysis of Satellite Data, Volume II - Radiation Analysis, Section 6. Fixed-Position Scanning - Tetsuya Fujita

30. Evaluation of Errors in the Graphical Rectification of Satellite Photographs - Tetsuya Fujita

31. Tables of Scan Nadir and Horizontal Angles - William D. Bonner

32. A Simplified Grid Technique for Determining Scan Lines Generated by the TIROS Scanning Radiometer - James E. Arnold

33. A Study of Cumulus Clouds over the Flagstaff Research Network with the Use of U-2 Photographs - Dorothy L. Bradbury and Tetsuya Fujita

34. The Scanning Printer and Its Application to Detailed Analysis of Satellite Radiation Data - Tetsuya Fujita

35. Synoptic Study of Cold Air Outbreak over the Mediterranean using Satellite Photographs and Radiation Data - Aasmund Rabbe and Tetsuya Fujita

36. Accurate Calibration of Doppler Winds for their use in the Computation of Mesoscale Wind Fields - Tetsuya Fujita

37. Proposed Operation of Intrumented Aircraft for Research on Moisture Fronts and Wake Depressions - Tetsuya Fujita and Dorothy L. Bradbury

38. Statistical and Kinematical Properties of the Low-level Jet Stream - William D. Bonner

39. The Illinois Tornadoes of 17 and 22 April 1963 - Joseph L. Goldman

40. Resolution of the Nimbus High Resolution Infrared Radiometer - Tetsuya Fujita and William R. Bandeen

41. On the Determination of the Exchange Coefficients in Convective Clouds - Rodger A. Brown

* Out of Print
** To be published

(Continued on back cover)

SMRP Research Paper No. 51

ERRATUM

Page 6 - On third line from bottom of page change Fujita and Fankhauser (1966) to Fujita, Wilk, and Fankhauser (1966).

Page 11 - References. Fourth reference should be _____, Kenneth E. Wilk, and James C. Fankhauser, 1966: A proposed explanation of deviate paths of echo couplets. Paper to be presented at the 12th Conference on Radar Meteorology at Norman, Oklahoma, Oct. 17-21, 1966.

SATELLITE AND MESOMETEOROLOGY RESEARCH PROJECT
Department of the Geophysical Sciences
The University of Chicago

FEATURES AND MOTIONS OF RADAR ECHOES ON PALM SUNDAY, 1965

by
Dorothy L. Bradbury and Tetsuya Fujita

(Chapter V of a Comprehensive Study of the Palm Sunday Tornadoes, 1965)

SMRP Research Paper #51
June 1966

The research presented in this paper has been sponsored by the Environmental Sciences Services Administration under grant Cwb WBG 70 (NSSL).

FEATURES AND MOTIONS OF RADAR ECHOES ON PALM SUNDAY, 1965[1]

Dorothy L. Bradbury and Tetsuya Fujita

Department of the Geophysical Sciences
The University of Chicago
Chicago, Illinois

ABSTRACT

An abundant amount of radar data gathered on Palm Sunday 1965 has been used to make a detailed study of the development of the tornado producing echoes. The echoes were matched with damage paths and reported time of occurrences, and then designated as separate tornado families. The rate and direction of motion of individual echoes were determined by plotting time-space positions of the echoes at 10 minute intervals from several radar stations.

A composite of radar photographs from three stations at intervals of from two minutes to ten minutes was used to show the growth rate and change in features of severe storm echoes.

Using the combined radar echoes from all available stations to supplement pressure, wind and dewpoint data, a detailed synoptic analysis was made for the period 11 through 23 CST. It was shown that the severe storm activity was associated with the advance of a dry cold front.

1. Introduction

For several years radar has been used as a basic tool for the study of the structure and motion of severe storms, including squall lines and tornadoes. It has been especially useful in research on tornadoes since the tornado producing echoes can be readily identified by matching the location of the echoes with the damage paths, visual reports, and photographs. One of the earlier studies on the motion of tornado producing echoes was made by Fujita (1958) using the Illinois tornadoes of 9 April 1953

---

[1]The research presented in this paper has been sponsored by the Environmental Science Services Administration under Grant Cwb WBG-70 (NSSL).

for the case study. A very detailed study on tornadoes with the use of radar has also been made of the 26 May 1963 tornadoes near Oklahoma City by Browning and Fujita (1965).

Because the Palm Sunday tornadoes of 1965 were so numerous and widespread and occurred over such a long period of time, approximately eleven hours, the opportunity was provided to make a detailed synoptic study using radar data to determine the rate and direction of motion of the individual storms as well as the change in the features of individual echoes. In order to get the best available radar coverage preceeding and during the outbreak of the numerous tornadoes of 11 April 1965 the radar film from the Weather Bureau operated WRS-57 radars within range of the storm area, the radar at Selfridge AF Base, Michigan, and the Illinois State Water Survey's CPS-9 were obtained. The Weather Bureau stations included Minneapolis, Des Moines, Chicago, Detroit, Evansville, Cincinnati, and Akron. In order to follow the cloud echoes, traces were made from the film onto grids for each station at approximately 10 minute intervals between the hours of 11 and 23 CST. Some of the radars were in operation during only part of this period and as the storm approached the station the radar was changed over to short range. This made it somewhat difficult to obtain complete coverage of the entire area. However, this difficulty was partially overcome since the radar ranges overlapped and the area eliminated by one station was picked up by another.

2. Tornado Families and their Parent Echoes.

When all available radar data were combined with information gathered from eye witness and newspaper reports (Chapt. 1) and aerial surveys (Chapt. II)[2] the time and location of the various tornadoes and their damage paths were reconstructed as accurately as possible. To study motions of the radar echoes the locations of individual echoes were plotted onto a base chart which included range markers for each radar station drawn as polar coordinates. In this manner the echo could be tracked from its inception to dissipation. By matching echo positions with damage paths the tornado producing echoes were separated from the non-producing echoes and assigned an identifying family letter as shown in figure 1.

The exact number of individual tornado funnels in such an intense outbreak as this case was difficult to determine. However, when the funnel path crossed over wooded regions, areas with farm buildings, and more densly populated areas the

---

[2]Chapter II appears as SMRP Research Paper No. 49.

destruction left in its wake outlined clearly its path (Chapt. II). Figure 1 shows the damage paths of the individual tornado families, the paths of the tornado cyclone echoes, and the approximate time of tornado occurrence. The numbers in parentheses indicate average speed of the echoes.

The complicated pattern of echo paths, damage paths, and reported time of tornado occurrences over northern Indiana and southern Michigan caused some difficulty in matching the echoes with times of tornado occurrence and the damage paths. Part of this difficulty was due to different elevation angles and gain settings of the various radars as well as the distance of the echoes from the stations. Also, in several cases, two or more echoes followed along almost the same path from thirty to fifty minutes apart. Thus to identify the damage with a specific echo was not easy. One such case is shown in figure 6a which is a composite of pictures from the radar film of the Illinois State Water Survey's CPS-9 taken at two minute intervals between 1624 and 1714 CST. The first echo of family J was picked up by the Illinois State Water Survey radar (CMI) and Chicago Weather Bureau's WRS-57 (CHI-F) at approximately 15 CST. By 1636 CST a new echo formed (family K) in almost the same location where the echo of family J had been at 1550 CST. This second echo followed along in nearly the same path as the first but slightly to the left of it. This accounts for the fact that some areas experienced two tornadoes within less than an hour and it also accounts for the especially wide damage path over southern Michigan where the two paths converged.

If one compares the paths of the cloud echoes with the damage paths (figure 1) it can be seen that they do not exactly coincide. This difference may be due to one of two reasons or both. Firstly, the cloud echoes were tracked by selecting a point (usually near the center) within the echo and following this point at ten minute intervals. Because of the change in size and shape of the echo within short intervals of time the relative position of the point with respect to the echo may not be exact. Secondly, and probably the more important factor, the position of the tornado funnel with respect to the entire echo changes with time. Previous studies (Fujita, 1965) have indicated that initially the tornado cyclone (hook echo) is usually formed in the right rear part of the echo. The tornado funnel may move around the periphery of the tornado cyclone and gradually diminish in intensity as it moves away from the maximum vorticity zone and a new funnel forms, or it may maintain its intensity and move in toward the center. In other cases the tornado funnel may form at the center of the rotating cloud and remain there during its life time.

Figure 2 illustrates the different categories of tornado damage paths proposed by Fujita. The upper diagram represents the parallel mode of damage paths and is the result of the tornado funnel moving around the periphery of the rotating cloud and gradually dissipating as a new funnel develops. The bottom diagram represents the series mode in which the tornado forms at the center of the rotating cloud and remains there throughout its lifetime. The middle diagram represents the combined mode in which the tornado starts out as a parallel mode type but gradually moves toward the center of the tornado cyclone and becomes a series mode type. Family B tornadoes appear to have been an example of the parallel mode while tornado families J and K started out in the parallel mode and turned into series mode and thus are designated combined mode. Family L is an example of the series mode.

3. Rate and Direction of Motion of Tornado Producing and Non-producing Echoes.

Fujita (1958) and Browning and Fujita (1965) have shown that as soon as a severe thunderstorm or tornado cyclone cloud begins rotation it tends to veer at an angle of about 25 degrees from its original direction of movement or from that of other echoes in the vicinity. Newton and Katz (1958) found that convective rainstorms on the average moved with an appreciable component to the right of the 700 mb wind direction. Others have also substantiated that severe weather phenomena tend to follow a path to the right of the direction of the middle tropospheric winds.

The available upper wind data during the period of the tornadic activity on Palm Sunday, 1965 was at 18 CST. At or near this hour at least five tornadoes were in existence. Figure 3 is a chart showing the contours at the 500 mb level and the direction of movement of all trackable radar echoes during a forty minute period centered at 18 CST. The tornadoes occurring at this time are indicated by the solid circles. In all cases of tornado producing echoes the motion was to the right of the direction of the 500 mb winds but the degree of veering was not the same in all cases. The maximum angle of veer was approximately 22 degrees. Those echoes which did not produce tornadoes or intense damage-producing thunderstorms moved generally in the direction of the streamlines of the 500 mb winds.

Between 12 and 15 CST the average movement of the dry cold front in the area of the tornado outbreaks was between 35 and 40 knots (figure 4) while that of the echoes was between 40 and 45 knots. The echoes and resulting tornadoes and severe thunderstorms appear to be closely associated with the advancing dry cold front. However, the longest time that the individual echoes could be tracked was approximately one

and one-half hours with the average just under one hour. Thus the resulting tornado damage paths were relatively short and interrupted.

Between 15 and 18 CST the average rate of movement of the dry cold front in the area with tornado outbreaks was around 40 knots while that of the echoes was between 55 and 60 knots. Since the rate of movement of the echoes was approximately 150 percent of that of the front they moved out much ahead of it. Then as the front advanced it would initiate another line of echoes which would follow along in almost the same path of the original echoes. It appears that once the tornado cyclone was initiated it was able to become self-perpetuating as long as it remained within an environment which was able to supply it with the proper ingredients.

Between 18 and 21 CST the maximum forward motion of the dry cold front had increased to approximately 50 knots while the echo speed remained between 50 and 60 knots. Thus by 21 CST the line of echoes and the front were nearly coincident as the severity of the storm began to decrease. Figure 5 shows the position of the dry cold front and the radar echoes in the vicinity of the front at three hour intervals between 12 and 21 CST. An area of solid echo over northeastern Iowa and southern Minnesota is not indicated in this chart since it was not necessarily associated with the forward advance of the dry front but was a consequence of overrunning warm moist air.

4. Change in Features of Radar Echoes.

As was stated previously, it was possible to follow isolated radar echoes of the intense storms over a long period of time. The rate of growth of an echo after first detection on radar was quite rapid but after reaching maximum intensity the shape usually changed more markedly than the size. Figure 6 is a composite of the radar pictures taken by the Illinois State Water Survey's CPS-9 between 1624 and 1714 CST on long range and 1716 and 1820 CST on short range. The sequence of pictures of echo family J (figure 6a) begins at 1624 CST (1 hr 24 min after first detection on radar) when the echo was near its maximum size and was beginning to form a hook. The hook echo is clearly outlined by 1638 but it maintained this shape for only a short period of time. The first funnel touchdown from this echo was reported at 1645 CST.

The rapid growth of echo family K from the time of its first detection at 1636 to hook formation at 1712 CST can be followed in figure 6a. Here again, the hook echo was observed about ten minutes before the first funnel was reported.

The CPS-9 was then shifted to short range (figure 6b) and the echoes of families

L and M were observed until 1820 CST. These two families of echoes appear to pass through the same metamorphosis from first detection on radar to maximum development. One interesting feature is the the echo splitting of family L around 1730 in which the original echo continued in the same direction of movement but the separated part moved to the left and dissipated by 1820 CST.

There were numerous radar pictures from the various stations which showed interesting features but only a few have been chosen for this report. Those chosen had nearly constant range, gain setting, and elevation angle over a relative long period of time. One such case was Akron, Ohio (CAK) and figure 7 is a composite of the radar pictures from CAK on long range between 2027 and 2150 CST and on short range between 2155 and 2225 CST. Figure 7a shows the growth and change in features of four echo families during a period of approximately one and one-half hours. One interesting feature is the space interval between the strong echoes of approximately 50 miles which suggests that the severe storms suppress the growth of any other convective activity within a range of 20 to 25 miles. Another eye-catching feature is the simultaneous and almost identical change in the features of echo families J and O between 2050 and 2110 CST. At 2155 CAK changed to short range and figure 7b shows some features of the echo family L as it approached the station. The most significant feature to be observed in this sequence is the clear spot or eye which can be seen between 2200 and 2205. The echo exhibited a hook at 2155 but changed to a clear eye by 2200 CST. This tornado produced the damage path which extended from a point south southwest of Oberlin to Strongsville, Ohio (see figure 20, Chapter II).[3]

Another continuous series of echoes is from Evansville, Indiana (EVV) and the composite picture is shown in figure 8. This series extends from 1700 CST to 2100 CST with a time interval of ten minutes between pictures. In this series as well as the previous ones there can be observed several cases of echo splitting and then the two echoes moving in different directions. This phenomenon is observed frequently now that there are so many radar pictures available from both operational and research stations. Further research on this phenomenon will be undertaken by Fujita, and Fankhauser (1966).

Figure 8 also illustrates the change with time of the distribution of the echoes. Between 1700 and 1900 CST the echoes maintained an isolated distribution and were

---

[3]Chapter II appears as SMRP Research Paper No. 49.

intense severe storms, but as the solar heating lessened the new echoes that formed in advance of the approaching cold front were less intense and merged to form large elongated echoes which moved with the rate of the advancing cold front.

Such time-space series of cloud echoes as these are a valuable aid to the study of the development of severe storms. As the number of radar stations increases it is hoped that in the future similar sequences would be available on days with numerous tornadoes in order that a comparison could be made in the sequence of events leading to their development.

5. Composite Radar Echoes as an Aid in Synoptic Analysis.

Surface charts were plotted and analyzed for each hour between 11 and 23 CST. Figures 9 to 20 show these charts which include the sea level isobar and isodrosotherm patterns, the combined radar echoes, and the reported surface winds (one full barb = 5 knots).

At 11 CST (figure 9) a well organized cyclone center was located over central Iowa with a warm moist tongue of air pushing north-northwestward up the Mississippi valley from southern Illinois and a relatively cool dry tongue moving north-northeastward from southern Kansas and Missouri. Scattered radar echoes were observed over north central Iowa and southern Minnisota to the north of the surface cyclone center. A second group of echoes extended across northern Illinois and Indiana and were associated with the weak east-west warm front in this area. Scattered shower activity was reported within this zone. A third group of echoes was observed over central Ohio and these accompanied a mesosystem that had moved from Missouri across central Illinois and Indiana during the morning. Moderate to heavy thunderstorm activity was reported in this area.

At 12 CST (figure 10) the cyclone center showed some intensification as it moved in an east-northeasterly direction at about 40 knots. The warm moist tongue pushed further northwestward into eastern Iowa, with the 60F isodrosotherm extending into the cyclone center. The zone of convective activity over northern Illinois and Indiana spread into southern Michigan while the activity in Ohio moved southeastward. The dry tongue pushing across Missouri was distinctly outlined as the clear area between two cloudy zones in the picture taken by TIROS IX as it passed over this area at 12h 41.3m CST (figures 5, 6, and 7 Chapt. IV).[4] The echoes labeled A and B were those which resulted in the first tornadoes of families A and B (figure 1) that were reported

---

[4]Chapter IV appears as SMRP Research Paper No. 50.

between 1230 and 1300 CST. During the next three hour period (figures 11, 12, and 13) the cyclone continued its movement in an east-northeasterly direction at approximately 40 knots and showed some intensification. The scattered echoes to the north of the cyclone center had become consolidated into a mass which covered a large area over southeastern Minnesota and west-central Wisconsin by 15 CST. In this area the warm moist air was overrunning cool moist air which resulted in a zone with near saturation from the ground to above 10,000 feet. Convective cells were embedded in this large echo but they could not be identified as individual cells within the solid echo. This zone reported continuous light rain during the afternoon (from hourly precipitation data). The line of echoes associated with the warm front moved northward and by 14 CST the line extended from Madison, Wisconsin to east of Grand Rapids, Michigan. By 15 CST (figure 13) as the frontal system began to occlude, the alignment of the echoes changed from west-east to northwest-southeast across Lake Michigan.

The most significant change that occurred during this period was the strengthening of the isodrosotherm gradient in east central Iowa. This was the result of the continued push northward of the dry tongue and its gradual narrowing as the moist tongue began to wrap around it and cut off the dry air. This may have been the trigger action necessary to set off the tornadic activity that began in this area near 13 CST. Between 13 and 15 CST tornado families A and B moved in a northeasterly direction across northeastern Iowa into southern Wisconsin. Tornado families C and D had their first touchdown between 14 and 15 CST.

By 16 CST (figure 14) the northern part of the cool dry tongue was completely separated from the southern portion; the axis of the latter became oriented in a north-east-southwest line while that of the former maintained a north-south orientation. The north-south line of echoes over northern Illinois and southern Wisconsin were associated with families B, C, D, E, F, and G. All these had relatively short, interrupted damage paths except for B which had a lifetime of approximately three hours.

Between 16 and 17 CST a new line of echoes appeared from east central Illinois to northwestern Indiana. From this line of echoes two new families of tornadoes, J and K, were spawned. The first echo of family J was picked up by the Chicago radar around 1510 CST but the first touchdown, as indicated by the damage path, was north of Knox, Indiana at approximately 1645 CST. The first echo of family K was picked up by CHI-F at 1640 CST and the first funnel touchdown was about 19 miles east of Valparaiso, Indiana at 1725 CST (figure 15). These two families followed almost identical paths and in the area where they converged near the Indiana-Michigan state

line an exceptionally wide path of destruction resulted.

The first echo of family L appeared at 17 CST over east central Illinois and the first funnel touched down ten miles southwest of Lafayette, Indiana at approximately 1755 CST (figure 16). This family consisted of six separate tornadoes which covered a distance of 274 miles in 4 hr 23 min or an average speed of approximately 62.5 mph. Within an hour another echo, family M, was picked up to the southeast of the location where L originated (figure 16).

Figures 16 through 18 show the progressive eastward movement of the line of echoes but by 20 CST the individual echoes were beginning to become consolidated into a solid line with little space between the severe thunderstorm echoes. The echo which resulted in the damage near Bay City, Michigan (tornado family N) is not shown on figure 18 because Detroit (DTW), the only radar station within range of this area, changed over to short range at this hour.

By 21 CST (figure 19) the strong isodrosotherm gradient existed only over southern Indiana and Illinois, where the dry front was moving eastward at approximately 25 knots. Here the echoes were in a solid line and were moving at nearly the same speed as the dry front. It was not possible to pick out individual intense thunderstorm echoes; however, no severe damage was reported in this area. Over the northern half of Ohio the echoes could still be identified and tracked as individual storms through 23 CST. Severe thunderstorms and a few scattered tornadoes were still occurring as shown in figures 19 and 20.

From this synoptic study it has been shown that in the case of the Palm Sunday 1965 tornadoes there appears to be a close association between the initiation of the tornadic activity and the advance of a cold dry front with a strong isodrosotherm gradient. The gradient along the front was as large as 20-25F/30 n.mi in some places.

6. Summary

The vast amount of radar data available for this study of the Palm Sunday 1965 tornadoes has shown that radar can be very useful in making a detailed synoptic analysis, especially when the storms occur within a range of several radars. By matching time and positions of the echoes on the radar film from two or more stations with observed or reported damage one can separate the tornado producing echoes from the non-producers. It was then possible to determine the direction of motion of these echoes, their growth rate, and the change in features with time. It could be

observed that the hook formed on an echo a short time before the funnel cloud was observed and it maintained the hook feature for only a very short time, less than 10 minutes.

It is hoped that similar studies can be made in the future on cases with numerous tornadoes in order to compare the distribution, direction of motion and change in features with time of the tornado producing echoes.

REFERENCES

Browning, K. A. and T. Fujita, 1965: A family outbreak of severe local storms - a comprehensive study of the storms in Oklahoma on 26 May 1963. Part 1. Special Reports No. 32. Air Force Cambridge Research Laboratories, Bedford, Mass. 346 pp.

Fujita, T., 1958: Mesoanalysis of the Illinois tornadoes of 9 April 1953. J. of Meteor. 15, pp. 288-296.

_____, 1965: Formation and steering mechanisms of tornado cyclones and associated hook echoes. Mon. Wea. Rev. 93, pp. 67-78

_____, and James C. Fankhauser, 1966: Split of a thunderstorm into anticyclonic and cyclonic storms and their motion as determined from numerical model experiments. SMRP Research Paper No. 62.

Newton, C. W. and S. Katz, 1958: Movement of large convective rainstorms in relation to winds aloft. Bull. Amer. Meteor. Soc. 39, pp. 129-143.

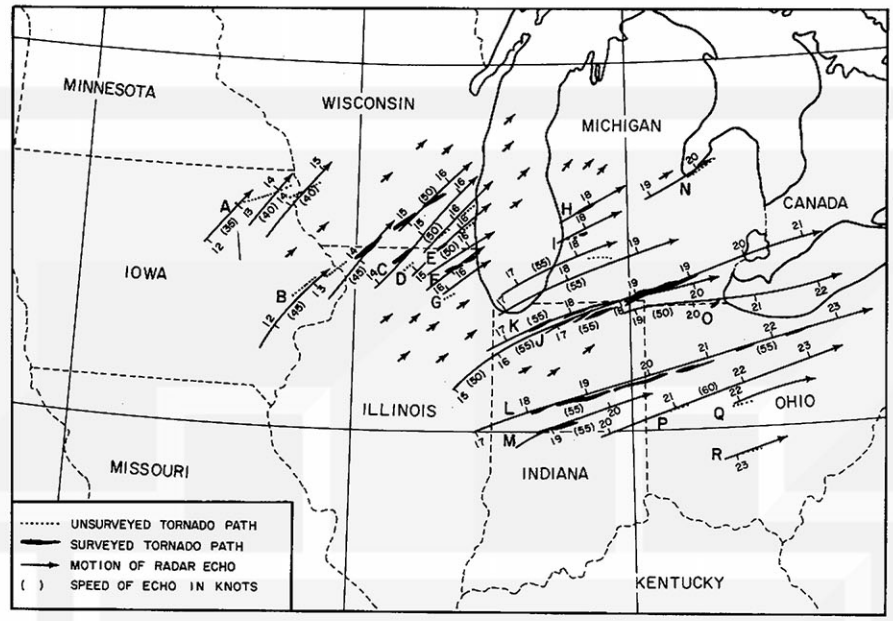

Figure 1. Chart shows aerial surveyed and unsurveyed tornado damage paths. Long lines with arrowheads represent direction of motion of damage producing echoes and short arrowheads are direction of motion of other echoes. The approximate time of occurrence (CST) is indicated at tick marks and numbers in parentheses are the average speed of the damage producing echoes. Letters A, B, C, etc. designate the individual tornado families.

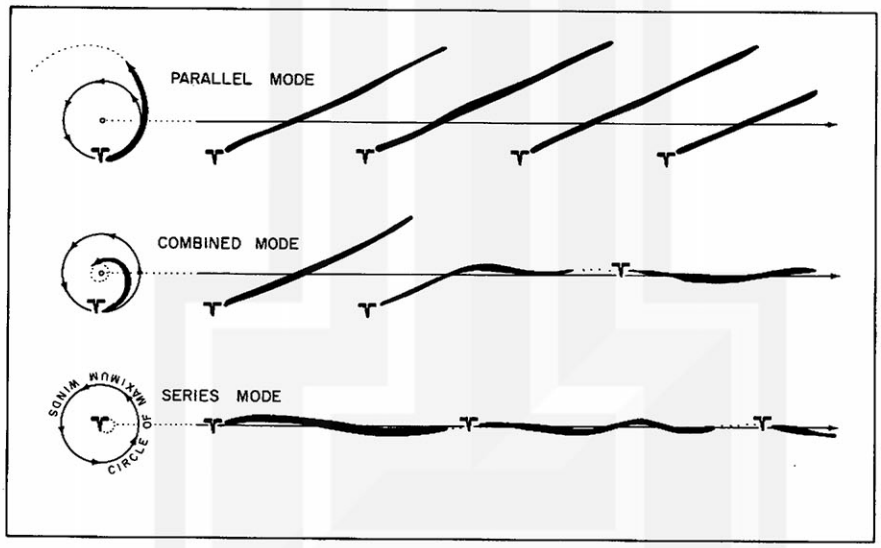

Figure 2. Categories of damage paths (extra thick lines) as proposed by Fujita. Upper diagram represents the parallel mode in which the tornado funnel forms near the rim of a rotating cloud and gradually moves away from the center of rotation and dissipates as a new funnel forms on the rim in the same relative position as the first one. The lower diagram represents the series mode in which the tornado funnel forms at the center of the rotating cloud and remains there during its lifetime. The middle diagram is a combination of the other two and is designated combined mode. In this type the tornado begins as a parallel mode and then changes into the series mode.

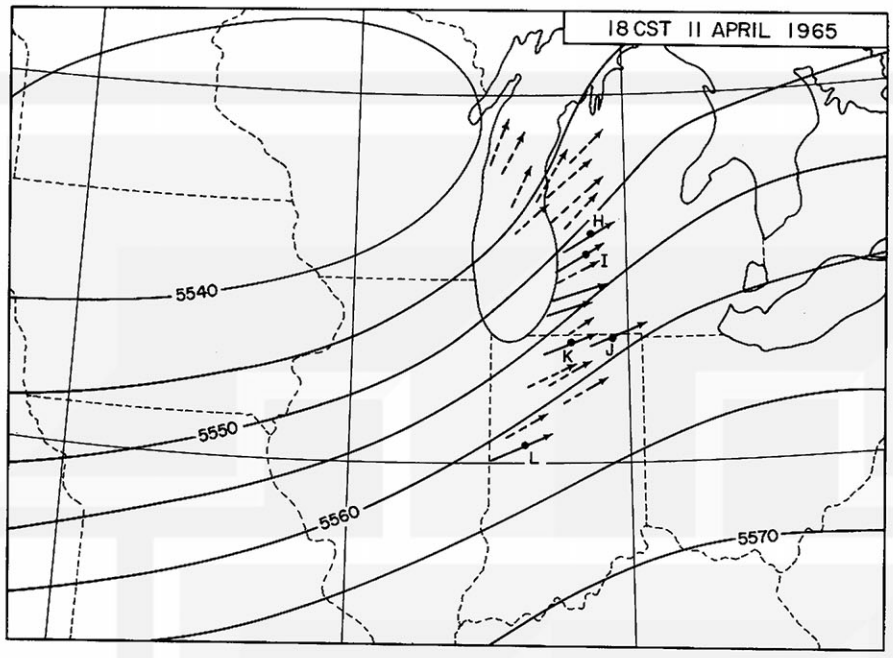

Figure 3. Chart shows 500-mb contours and direction of motion of damage producing (solid line arrow) and nonproducing (broken line arrow) echoes at 18 CST on 11 April 1965. Solid circles represent position of tornadoes in existence at this time.

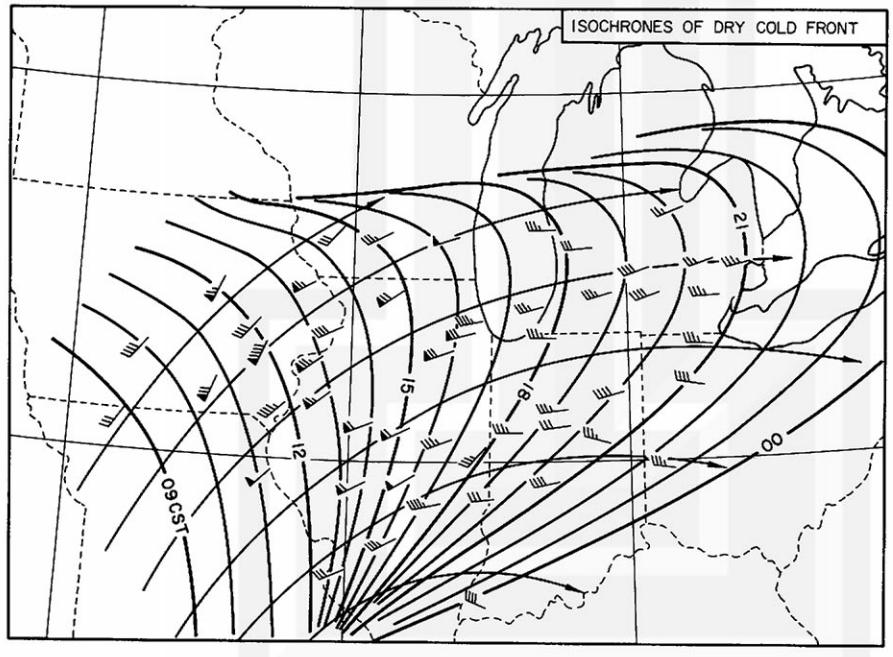

Figure 4. Isochrones of dry cold front are represented by heavy solid lines. Plotted surface winds (1 full barb = 5 knots) are those reported after the wind shift which accompanied the frontal passage. Fine lines with arrowheads represent the streamlines of these winds.

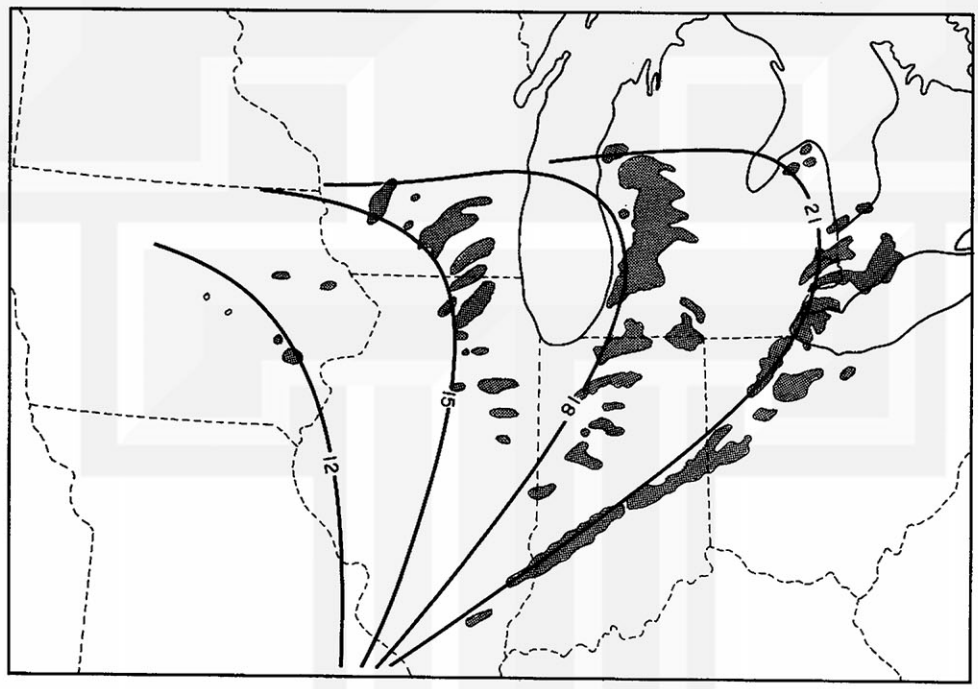

Figure 5. Three-hour positions of dry cold front are indicated by heavy solid lines. Stippled areas are radar echoes associated with the advancing front.

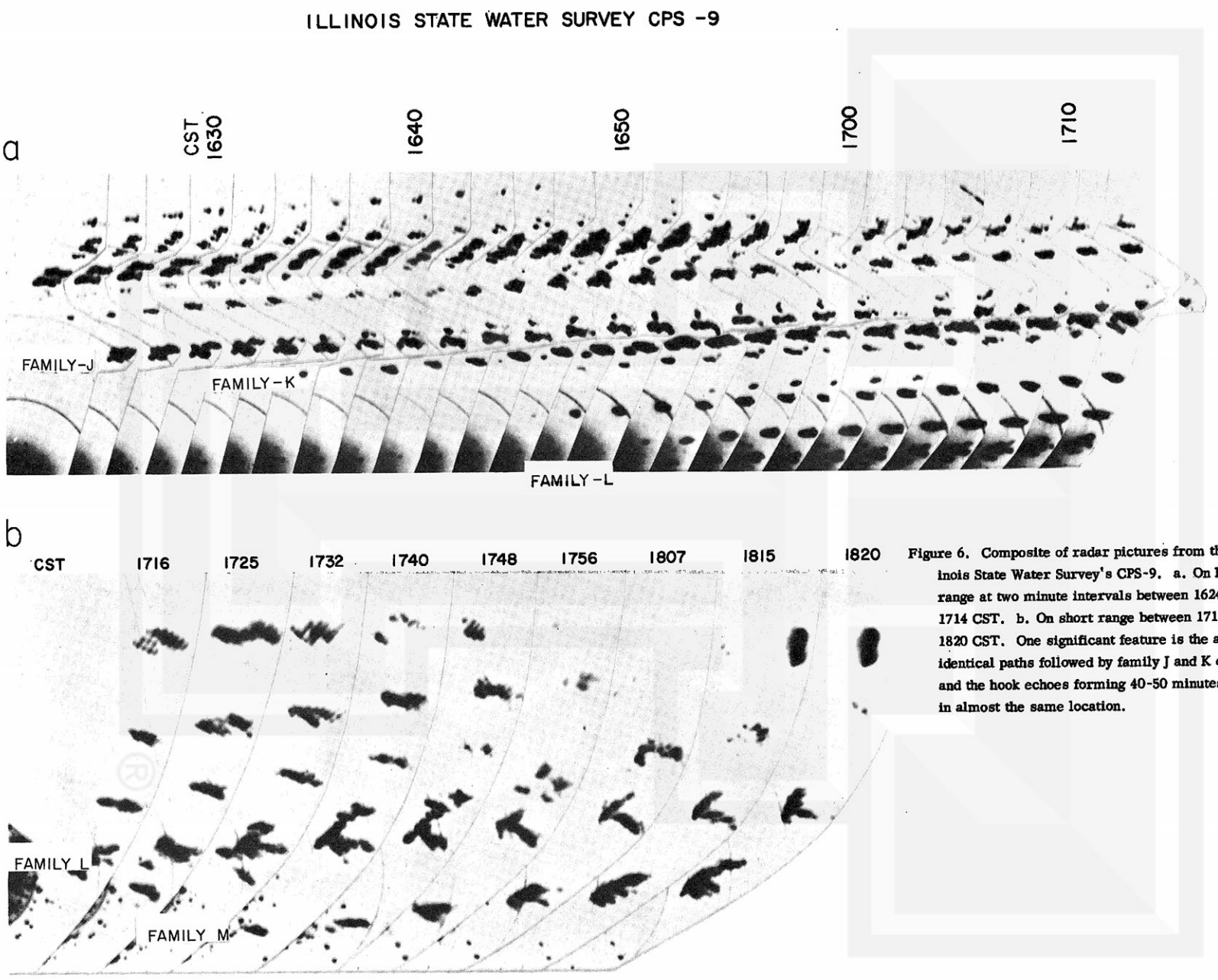

Figure 6. Composite of radar pictures from the Illinois State Water Survey's CPS-9. a. On long range at two minute intervals between 1624 and 1714 CST. b. On short range between 1716 and 1820 CST. One significant feature is the almost identical paths followed by family J and K echoes and the hook echoes forming 40-50 minutes apart in almost the same location.

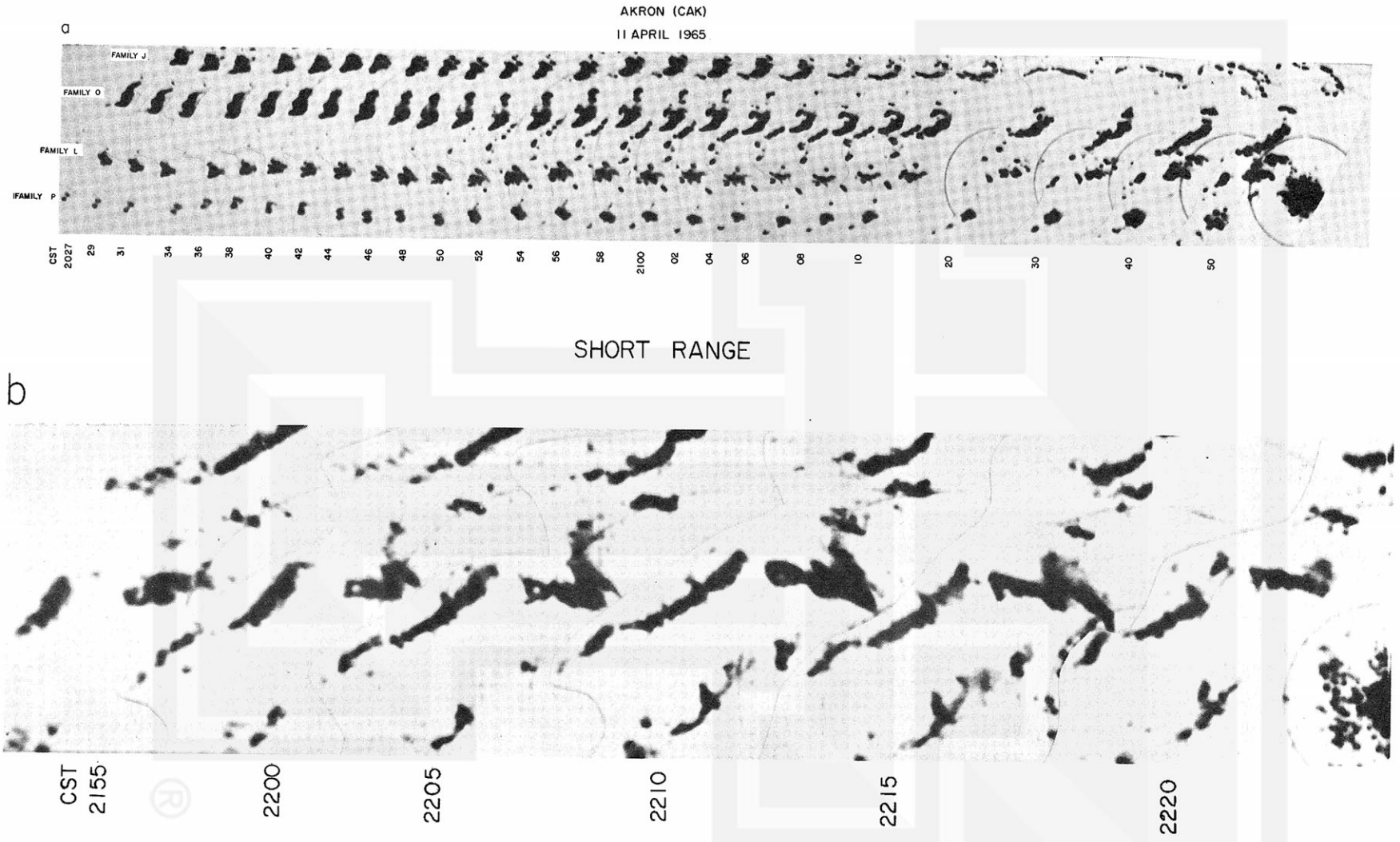

Figure 7. Composite of radar pictures from Akron's Decca 41 (CAK). a. On long range between 2027 and 2150 CST the change in the features of the echoes of four tornado families are shown. One outstanding feature is the almost simultaneous and almost identical change in the echoes of families J and O between 2050 and 2110 CST. b. On short range between 2155 and 2220 CST the significant feature is the tornado eye which appears as the clear spot in the echo near the 40-mile range marker.

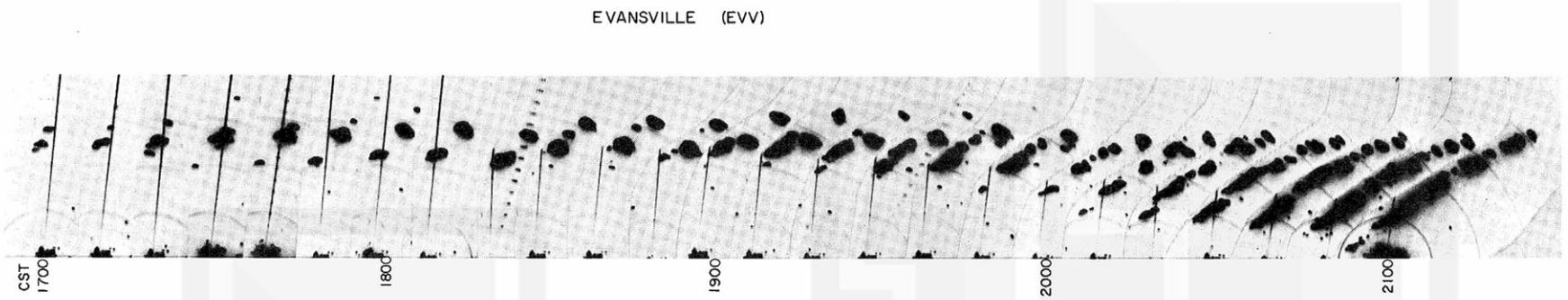

Figure 8. Composite of radar pictures from Evansville (EVV) at 10-minute intervals for the 4-hour period between 17 and 21 CST. The transition from isolated echoes to an almost solid line echo is clearly shown as the intensity of the storm decreases.

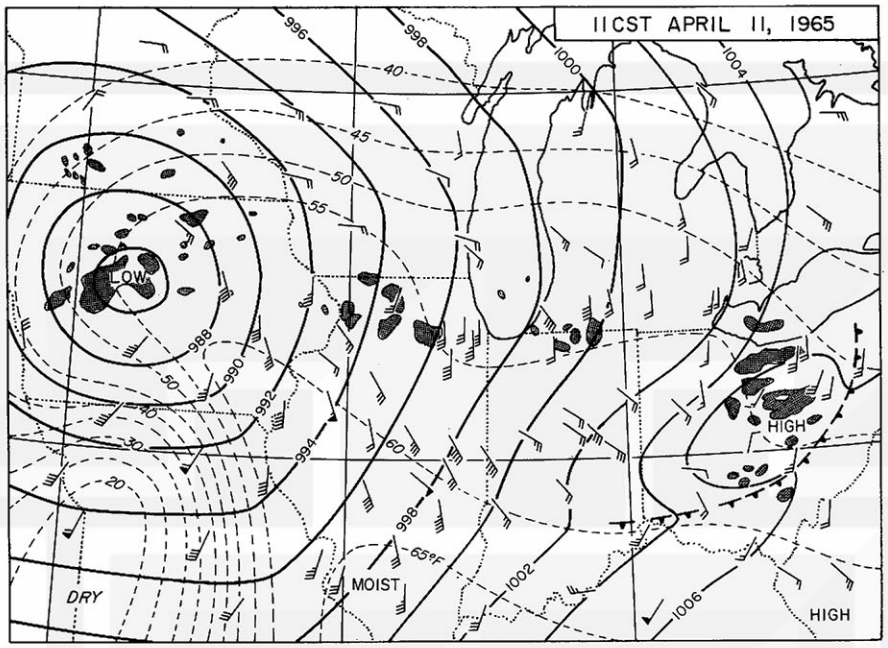

Figure 9. Surface chart with sea level isobars, isodrosotherms (degrees F), and winds (1 full barb = 5 knots) at 11 CST on 11 April 1965. Stippled areas indicate radar echoes. Note the dry tongue pushing northward from Kansas and Missouri and the moist tongue over southern Illinois.

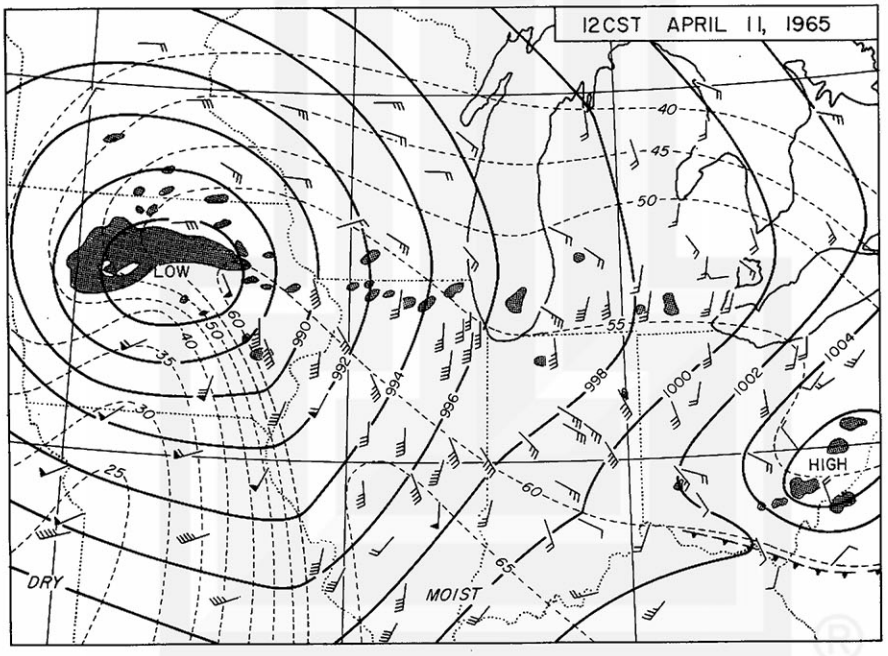

Figure 10. Surface chart with sea level isobars, isodrosotherms (degrees F), and winds (1 full barb = 5 knots) at 12 CST. Stippled areas indicate radar echoes. Note the strengthening of the isodrosotherm gradient over central Iowa.

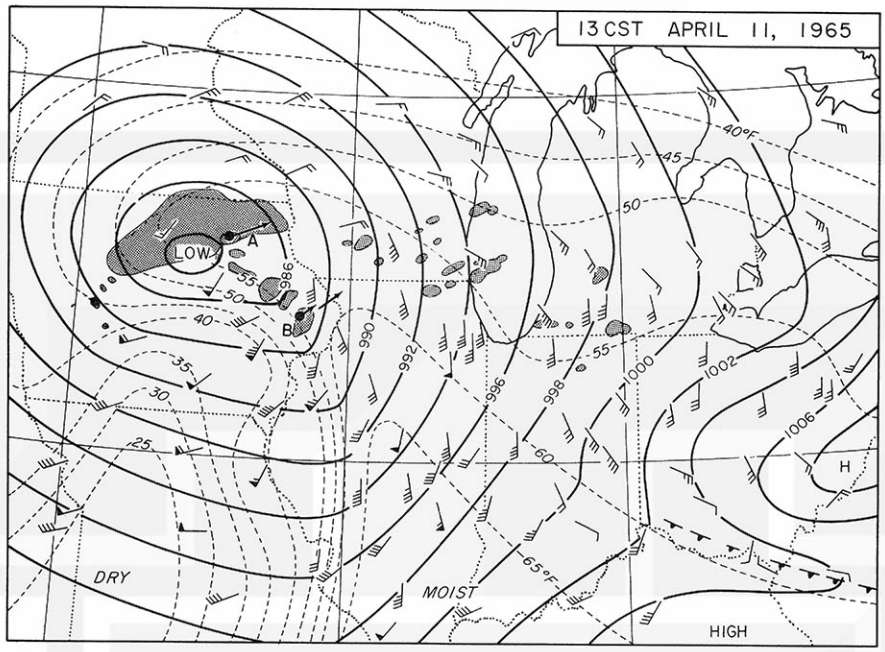

Figure 11. Surface chart with sea level isobars, isodrosotherms (degrees F), and winds (1 full barb = 5 knots) at 13 CST. Stippled areas indicate radar echoes. The large solid echo over northern Iowa is the result of warm moist air overrunning and is an indication of the continuous light rain reported in this area. The solid circles represent tornadoes that were on the ground at or near this time and the arrows represent the direction of motion of the tornado cyclone echo.

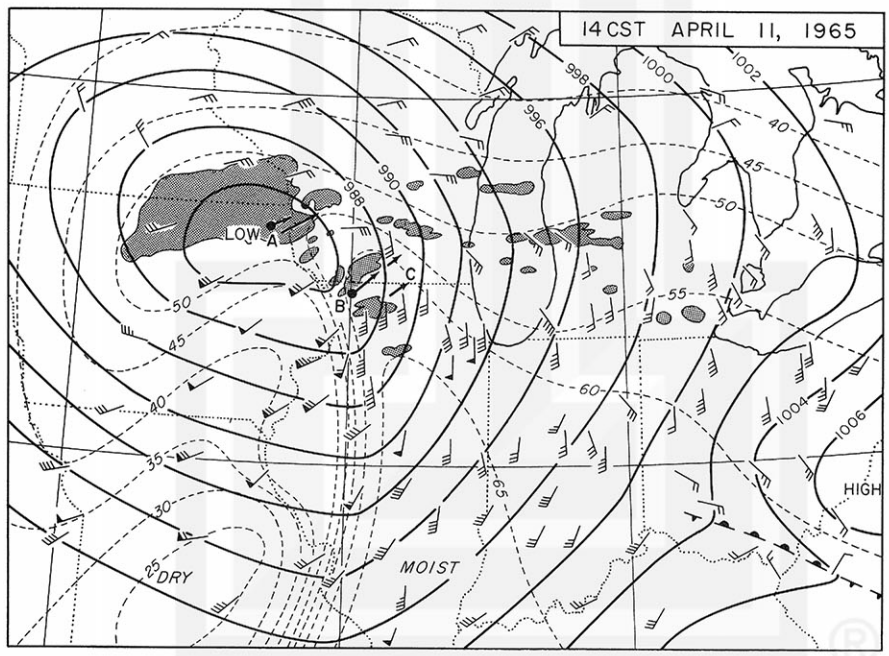

Figure 12. Surface chart with sea level isobars, isodrosotherms (degrees F), and winds (1 full barb = 5 knots) at 14 CST. Stippled areas represent radar echoes and solid circles indicates location of tornadoes on ground at map time. Arrows represent direction of motion of tornado cyclone echoes. Note especially the strengthening of the isodrosotherm gradient over west central Illinois.

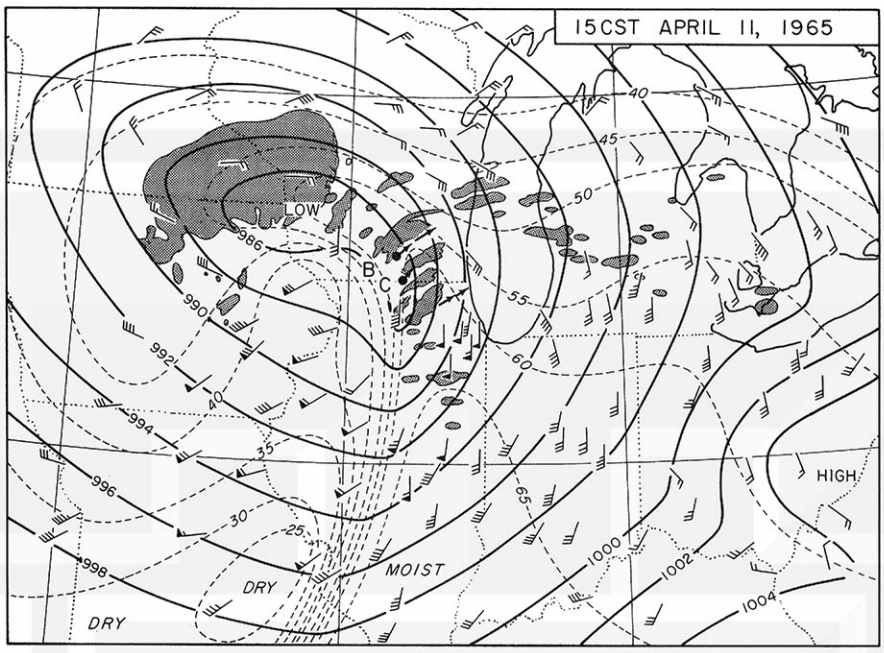

Figure 13. Surface chart with sea level isobars, isodrosotherms (degrees F), and winds (1 full barb = 5 knots) at 15 CST. Stippled areas indicate radar echoes and solid circles are tornadoes on the ground at map time. Arrows show direction of motion of tornado cyclone echoes. The band of strong isodrosotherm gradient has moved eastward to central Illinois and extends almost the full length of the state.

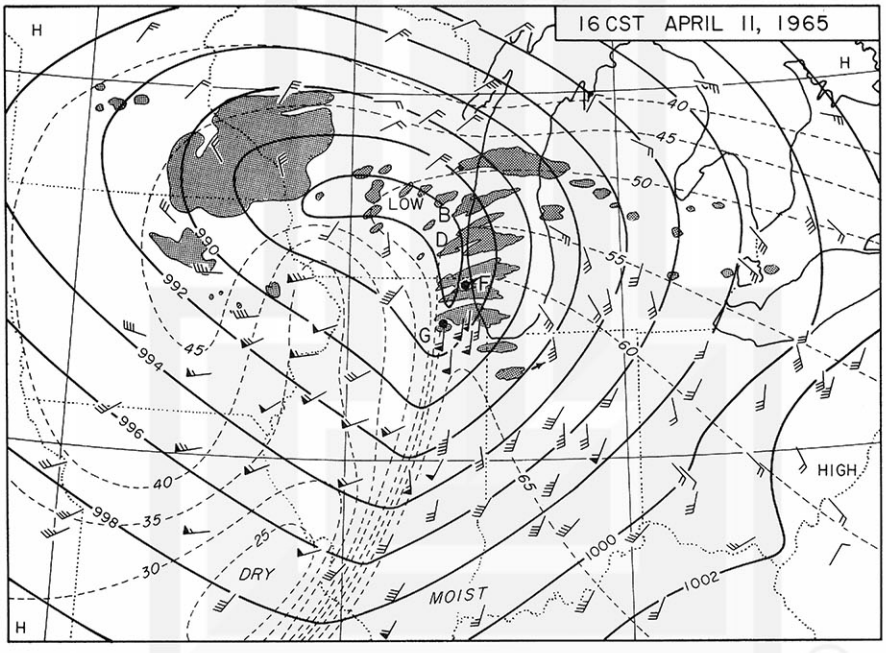

Figure 14. Surface chart with sea level isobars, isodrosotherms (degrees F), and winds (1 full barb = 5 knots) at 16 CST. Stippled areas represent radar echoes. Solid circles represent tornadoes on the ground at map time and arrows the direction of motion of tornado cyclone echoes. The northern part of the dry tongue is being narrowed and gradually cut off from the southern portion.

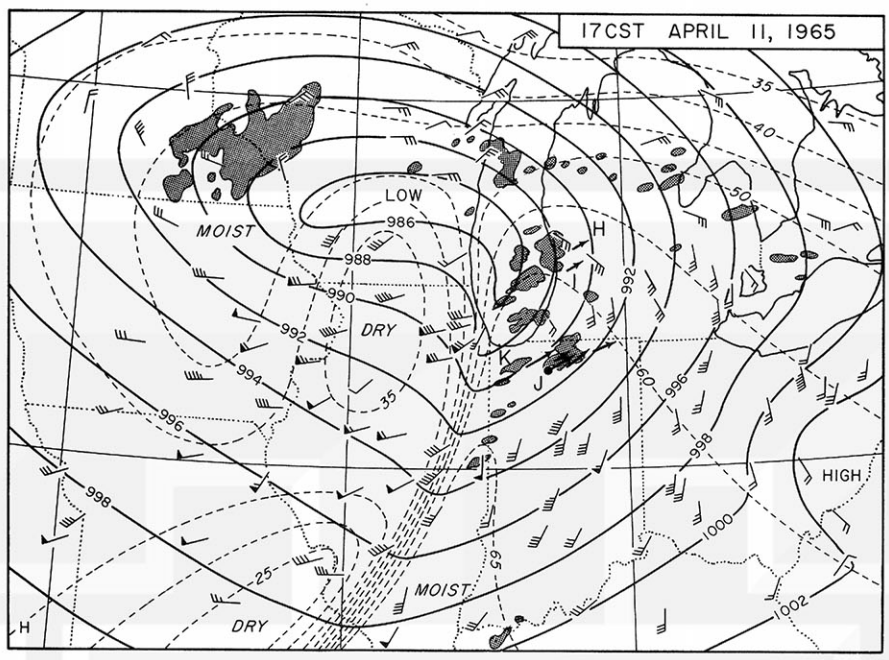

Figure 15. Surface chart with sea level isobars, isodrosotherms (degrees F), and winds (1 full barb = 5 knots) at 17 CST. Stippled areas represent radar echoes, arrows are the direction of motion of tornado cyclone echoes, and the solid circle is the location of the tornado of family J that was on the ground at map time. The tornado cyclone of family J has moved much faster than the dry front (represented by isodrosotherm gradient) which initiated it and a new line of echoes has formed just ahead of the front.

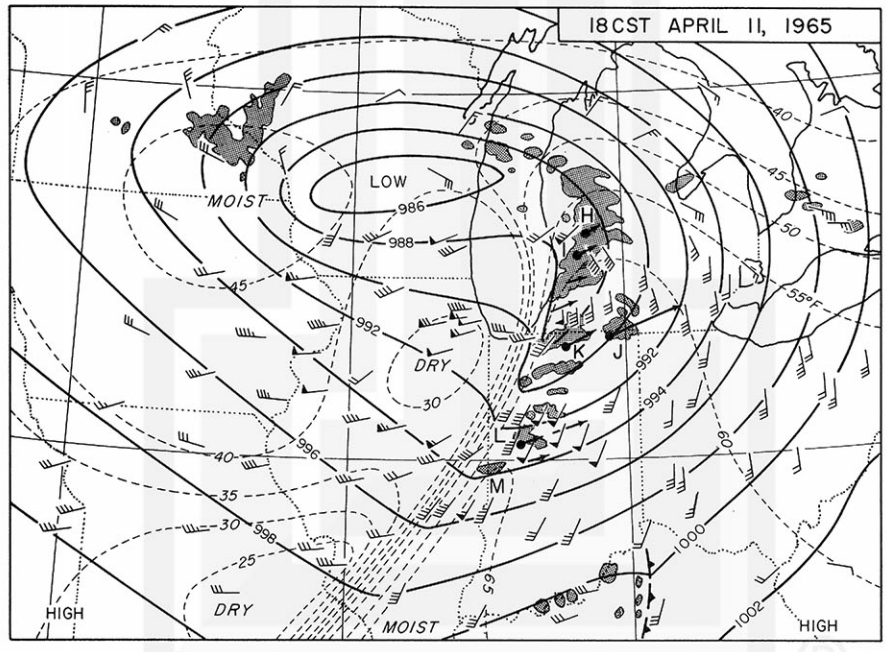

Figure 16. Surface chart with sea level isobars, isodrosotherms (degrees F), and winds (1 full barb = 5 knots) at 18 CST. Stippled areas represent radar echoes, arrows are the direction of motion of tornado cyclone echoes, and solid circles are the location of tornadoes on the ground at map time. Note that the direction of motion of the echoes of families J and K are almost parallel and that their paths are nearly coincident.

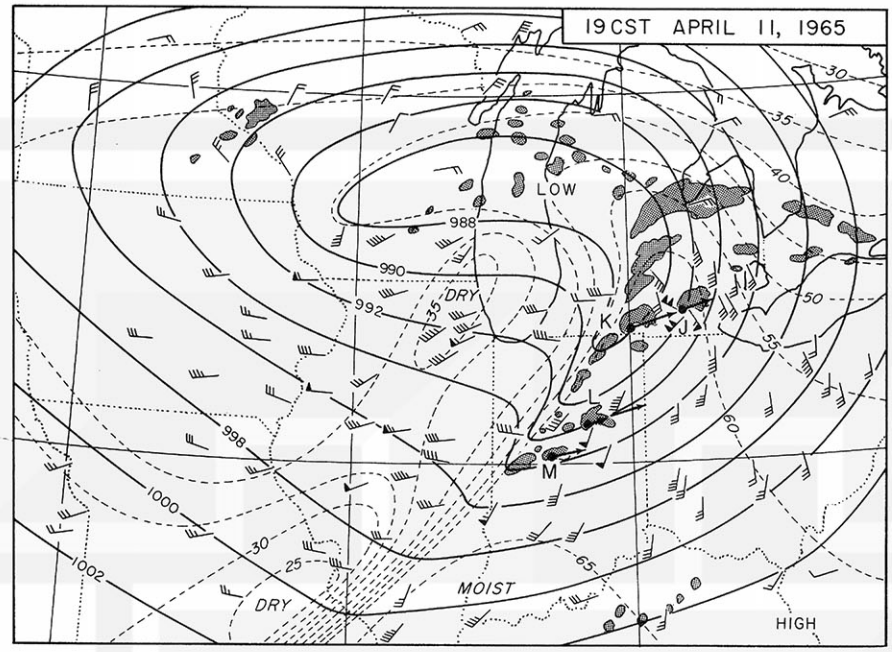

Figure 17. Surface chart with sea level isobars, isodrosotherms (degrees F), and winds (1 full barb = 5 knots) at 19 CST. Stippled areas represent radar echoes, arrows are the direction of motion of tornado cyclone echoes, and solid circles are the location of tornadoes on the ground at map time. New tornado outbreaks during the hour have been families L and M over central Indiana. The northern part of the dry tongue has been cut off and the isodrosotherm gradient over northern Indiana and southern Michigan is weakening.

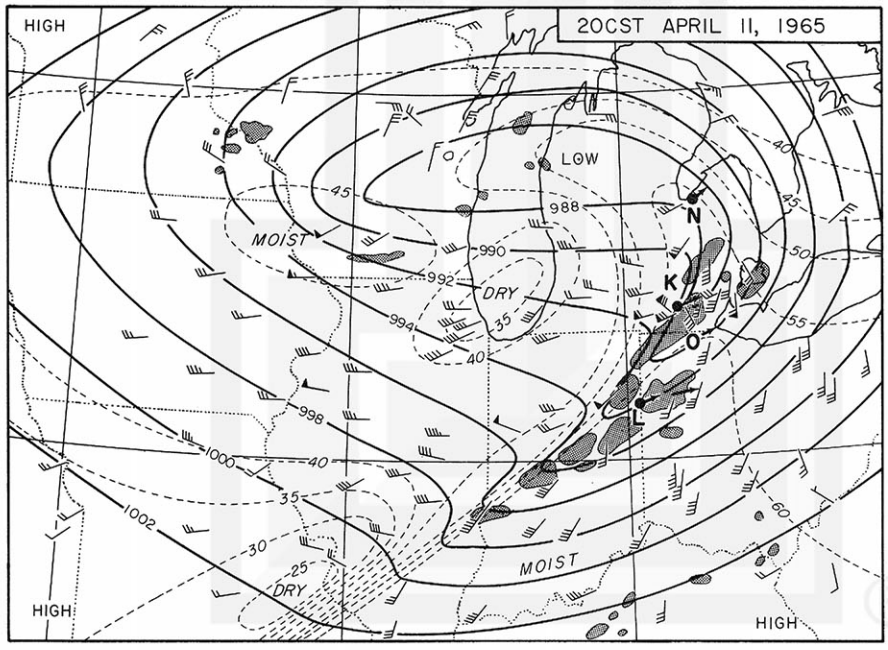

Figure 18. Surface chart with sea level isobars, isodrosotherms (degrees F), and winds (1 full barb = 5 knots) at 20 CST. Stippled areas represent radar echoes, arrows are direction of motion of tornado cyclone echoes, and solid circles are the location of tornadoes on the ground at map time. The echoes associated with tornado family N are missing since the Detriot radar switched over to short range at this time and no other station was within range.

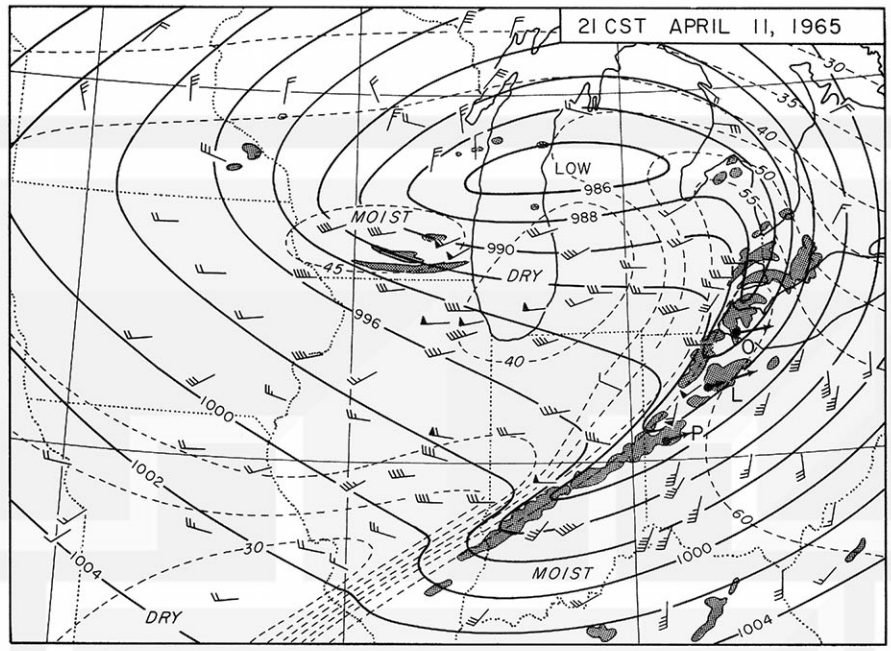

Figure 19. Surface chart with sea level isobars, isodrosotherms (degrees F), and winds (1 full barb = 5 knots) at 21 CST. Stippled areas represent radar echoes, arrows are direction of motion of tornado cyclone echoes, and solid circles are the location of tornadoes on the ground at map time. As the strength of the isodrosotherm gradient has weakened the echoes have become consolidated into elongated masses instead of individual isolated units.

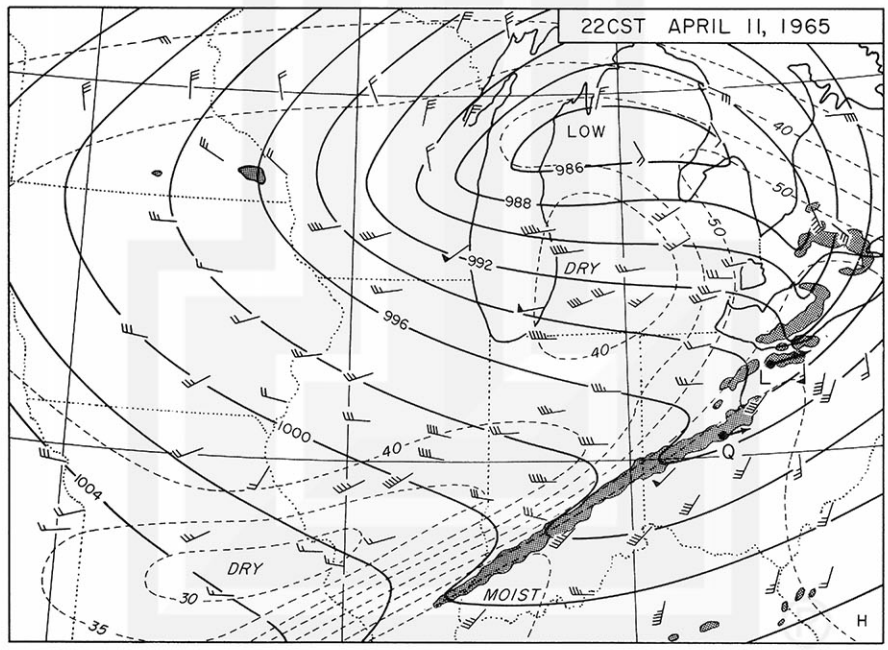

Figure 20. Surface chart with sea level isobars, isodrosotherms (degrees F), and winds (1 full barb = 5 knots) at 22 CST. Stippled area represents radar echoes, arrows are direction of motion of tornado cyclone echoes, and solid circles are the location of tornadoes on the ground at map time.

MESOMETEOROLOGY PROJECT - - - RESEARCH PAPERS

(Continued from front cover)

42. A Study of Factors Contributing to Dissipation of Energy in a Developing Cumulonimbus - Rodger A. Brown and Tetsuya Fujita

43. A Program for Computer Gridding of Satellite Photographs for Mesoscale Research - William D. Bonner

44. Comparison of Grassland Surface Temperatures Measured by TIROS VII and Airborne Radiometers under Clear Sky and Cirriform Cloud Conditions - Ronald M. Reap

45. Death Valley Temperature Analysis Utilizing Nimbus I Infrared Data and Ground-Based Measurements - Ronald M. Reap and Tetsuya Fujita

46. On the "Thunderstorm - High Controversy" - Rodger A. Brown

47. Application of Precise Fujita Method on Nimbus I Photo Gridding - Lt. Cmd. Ruben Nasta

48. A Proposed Method of Estimating Cloud-top Temperature, Cloud Cover, and Emissivity and Whiteness of Clouds from Short- and Long-wave Radiation Data Obtained by TIROS Scanning Radiometers - T. Fujita and H. Grandoso

49. Aerial Survey of the Palm Sunday Tornadoes of April 11, 1965 - Tetsuya Fujita

50. Early Stage of Tornado Development as Revealed by Satellite Photographs - Tetsuya Fujita